Journal of Translational Medicine

RESEARCH

Open Access

Quadrant asymmetry alteration of deep retinal capillary plexus degeneration in pathological myopia

Yilei Shao[1,2,3], Meixiao Shen[1,2,3], Fan Lu[1,3] and Jie Ye[1,2,3*]

Abstract

Background To measure quadrant asymmetry (QA) alterations of macular retinal microvascular density and determine their effect on pathological myopia.

Methods Optical coherence tomography angiography (OCTA) images of 20 control, 42 simple high myopia and 20 pathological myopia eyes were analyzed to quantify the density of the macular retinal microvascular network that included the superficial and deep retinal capillary plexuses (SRCP and DRCP). The definition of QA was calculated by subtracting the minimum value from the maximum value among the four macular respective subfields. The comparison of the QAs of SRCP and DRCP density among the three groups and the effect of QAs on the occurrence of pathological myopia were analyzed.

Results In pathological myopia, densities of the SRCP and DRCP were lower than in simple high myopia and control ($P < 0.05$). The higher QAs of SRCP and DRCP density occurred in pathological myopia than in simple high myopia and control ($P < 0.05$). In multivariate binary logistic regression, higher QA of DRCP density was associated significantly with the occurrence of pathological myopia (Odds Ratio = 2.000, $P = 0.035$) while the QA of SRCP density didn't ($P = 0.065$). Comparing the intra-quadrant effect on the occurrence of pathological myopia with the analysis of binary multivariate logistic regression, the decreased DRCP density in the macular inferior subfield showed a high risk (Odds Ratio = 0.435, $P = 0.030$).

Conclusions The occurrence of pathological myopia affected the quadrant asymmetry alterations of macular retinal microvascular density, especially the increased QA of DRCP density with significantly decreased DRCP density in the macular inferior subfield.

*Correspondence:
Jie Ye
jieyeah8651@wmu.edu.cn
[1]National Clinical Research Center for Ocular Diseases, Eye Hospital, Wenzhou Medical University, Wenzhou, China
[2]State Key Laboratory of Eye Health, Eye Hospital, Wenzhou Medical University, Wenzhou, China
[3]School of Ophthalmology and Optometry and Eye Hospital, Wenzhou Medical University, 270 Xueyuan Road, Wenzhou 325027, Zhejiang, China

Introductions

With the increasing prevalence of myopia, high myopia had become common worldwide, especially in Asian countries [1]. During the progression of high myopia, it was predicted that nearly 40.6% of high myopia would result in pathological myopia with a high risk of visual impairment [2–4]. Pathological myopia had been considered as one of the major causes of vision loss [5]. It was important to understand the risks and potential mechanisms for pathological myopia to the early screening, detection and treatment in the daily clinics.

The pathological myopia was considered to be highly associated with the degeneration of retinal microvasculature [6–8]. Our previous studies had demonstrated the decreased retinal microvascular perfusion in pathological myopia and were associated with visual impairment both in macular and peripapillary areas [6, 9]. The different alterations of retinal microvascular perfusion in peripapillary subfields had been reported with decreased retinal microvascular perfusion in tempo-inferior peripapillary subfield as the protective mechanism to visual impairment [9]. As we had known, the large blood vessels around the peripapillary area sent the branches to the macular regions. Whether there was also any quadrant asymmetric alteration of the retinal microvascular perfusion in the macular area was still unclarified. It had been found that decreased retinal microvascular density in all macular subfields in high myopia except the superior-temporal area [7].

The parameter of quadrant asymmetry (QA) was sensitive to indicate the quadrant asymmetric alteration of the retinal microvascular perfusion in various retinal diseases, and even predict the severity of the related diseases [10–12]. What's more, we had already developed custom algorithms that could identify the density of the retinal microvasculature with optical coherence tomography angiography (OCTA) images automatically [6, 13]. In the current study, we would like to evaluate the quadrant asymmetric change in the macular retinal microvascular perfusion with OCTA images in high myopia, especially in pathological myopia. We would also assess these changes with the occurrence of pathological myopia.

Methods

Subjects

The current study was a prospective, cross-sectional study. All subjects were recruited from August 2017 to May 2018 at the Eye Hospital of Wenzhou Medical University, Wenzhou, China. This study was approved by the Ethics Committee of the Eye Hospital of Wenzhou Medical University, Wenzhou, China, in accordance with the tenets of the Declaration of Helsinki.

The enrolled subjects were divided into three groups: (1) control (spherical equivalent [SE] -1.0 diopter [D] to +0.5 D), (2) simple high myopia (SE ≤ -6.0 D or axial length [AL] ≥ 26.5 mm without pathological changes in the fundus), and (3) pathological myopia (SE ≤ -6.0 D or AL ≥ 26.5 mm with pathological changes in fundus). According to the International Meta-Analysis for Pathological Myopia (META-PM) classification system, high myopic eyes only with tessellated fundus or without any macular lesion were considered as simple high myopia, while high myopic eyes with diffuse chorioretinal atrophy, patchy chorioretinal atrophy, or macular atrophy were considered as pathological myopia [3]. Those with intraocular pressure (IOP) > 21 mmHg, age-related macular degeneration, significant cataract, diabetic retinopathy, history of intraocular surgery, serious complications of high myopia such as retinal detachment, or related systemic diseases were excluded from the current study.

Clinical examinations

All included subjects were asked to undergo comprehensive clinical examinations, including refractive error with best corrected visual acuity (BCVA, measured as Snellen acuity), slit lamp biomicroscopy, AL (measured by the IOL Master [Carl Zeiss, Jena, Germany]), non-contact IOP (measured by the Full Auto Tonometer TX-F [Topcon, Tokyo, Japan]), and fundus photography with a 45-degree digital retinal camera (Canon EOS 10D SLR backing; Canon, Inc., Tokyo, Japan).

Image Acquisition Protocol and Analysis

All enrolled subjects were imaged by OCTA (Optovue RTVue XR Avanti; Optovue, Inc., Fremont, CA, USA) to obtain retinal OCTA images. The scan speed was 70,000 A-scans per second. The OCTA images were obtained by orthogonal registration and merging of two consecutive 3 × 3 mm scans centered on the fovea. Good sets of scans with a scan quality of more than 4/10 (defined by the machine itself) were selected for further analysis.

All OCTA images obtained were corrected for magnification based on the AL using Bennett's formula, which had been described in detail in our previous studies [6, 13]. Custom-developed software was then used to quantify the vessel densities of the superficial retinal capillary plexus (SRCP) and the deep retinal capillary plexus (DRCP) [6]. The SRCP was extended from the internal limiting membrane to 10 μm below the inner plexiform layer (IPL). The DRCP was extended from 10 μm below the IPL to 10 μm below the outer plexiform layer (OPL). For each OCTA image, the densities of SRCP and DRCP were automatically calculated for the 2.5-mm diameter parafoveal region, excluding the foveal avascular zone within a circle of fixed radius (diameter = 0.6 mm) at the center of the macular fovea (Fig. 1).

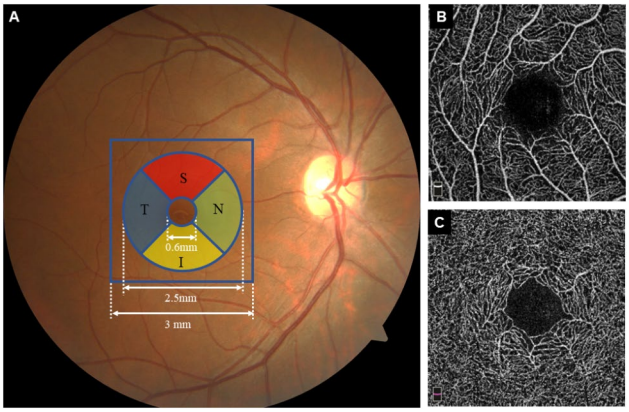

Fig. 1 Macular regions analyzed by OCTA with macular angio 3 × 3 mm scanning mode. (**A**) The analyzed macular area was 2.5-mm diameter parafoveal region, excluding the foveal avascular zone within a circle of fixed radius (diameter = 0.6 mm) at the center of the macular fovea. Then the analyzed area was further divided into four subfields: inferior (I), nasal (N), superior (S), temporal (T). (**B**) The OCTA image of SRCP; (**C**) The OCTA image of DRCP. OCTA, optical coherence tomography angiography; SRCP, superficial retinal capillary plexuses; DRCP, deep retinal capillary plexuses

The analyzed macular area was further divided into four subfields for all OCTA images, e.g., inferior, nasal, superior, and temporal. The definition of QA was calculated by subtracting the minimum value from the maximum value among the four respective subfields [10].

Statistical analyses

All data were analyzed with SPSS software (version 22.0; SPSS, Inc., Chicago, IL, USA) and calculated as means ± standard deviations. The SE of refraction error was analyzed as the spherical dioptric power plus one-half of the cylindrical dioptric power. The BCVA was converted into the logarithm of the minimum angle of resolution (logMAR) for analysis. One-way analysis of variance (ANOVA) was used to compare the differences among the three groups, and post hoc procedures were used to compare differences between every two groups. Differences in gender ratios among the three groups were analyzed by the χ^2 test. The independent samples t-test was used to calculate and compare the mean difference in QA between every two groups. The binary logistic regression based on generalized estimating equation (GEE) analysis was performed to identify the effect of QA of retinal microvasculature density on pathological myopia and also the effect of retinal microvasculature density in subfields on pathological myopia. The cumulative distribution function was plotted to perform the QA of retinal microvasculature density among the three groups. The P-values less than 0.05 were considered statistically significant.

Results

Basic patient characteristics

There were no significant differences in gender ratio, age, or IOP among the control, simple high myopia and pathological myopia ($P = 0.453$, 0.066, and 0.172, respectively, Table 1). The significant difference in AL, SE and BCVA occurred among the three groups (All $P < 0.001$, Table 1). Compared to simple high myopia and controls, pathological myopia had greater refractive errors, worse BCVA, and longer AL ($P < 0.001$ for all, Table 1). However, there was no significant difference in BCVA between the controls and simple high myopia ($P = 0.173$, Table 1).

Differences in retinal microvasculature density among the control, simple high myopia and pathological myopia

For the SRCP density, there was a significant difference among the three groups not only in the global area but also in the four respective subfields ($P \le 0.003$, Table 2). However, there was only a significant difference in SRCP density in the global area and temporal area between simple high myopia and pathological myopia ($P = 0.012$ and 0.007, respectively, Table 2) but not in the other three subfields (All $P > 0.05$, Table 2).

For the DRCP density, there was a significant difference among the three groups not only in the global area but also in the four respective subfields (All $P \le 0.001$, Table 2). A significant difference in DRCP density was also found between simple high myopia and pathological myopia in global and all four respective subfields (All $P \le 0.033$, Table 2).

Table 1 Basic characteristics of the three groups

Parameters	Control	Simple high myopia	Pathological myopia	P^*	P_1	P_2	P_3
N	20	42	20	-	-	-	-
Age, year	38.2 ± 13.5	32.2 ± 9.51	37.7 ± 11.5	0.066	0.144	1.000	0.210
Gender, F:M	14:6	27:15	16:4	0.453	0.777	0.716	0.252
AL, mm	23.98 ± 0.69	27.5 ± 1.17	29.17 ± 1.28	< 0.001	< 0.001	< 0.001	< 0.001
SE, diopter	-0.49 ± 0.69	-10.33 ± 2.74	-13.49 ± 3.14	< 0.001	< 0.001	< 0.001	< 0.001
IOP, mmHg	14.69 ± 3.96	16.32 ± 2.41	14.82 ± 4.19	0.172	0.117	0.912	0.133
BCVA, LogMAR (Snellen Acuity)	-0.01 ± 0.04 (20/20)	0.02 ± 0.03 (20/20)	0.15 ± 0.16 (20/32)	< 0.001	0.173	< 0.001	< 0.001

–, not performed; F, female; M, male; AL, axial length; SE, spherical equivalent; IOP, intraocular pressure; BCVA, best corrected visual acuity. P^*, P value among the three groups; P_1, P value between control group and simple high myopia; P_2, P value between control group and pathological myopia; P_3, P value between simple high myopia and pathological myopia.

Table 2 Differences in retinal microvasculature density between patients among the control, simple high myopia and pathological myopia

Parameters	Control	Simple high myopia	Pathological myopia	P^*	P_1	P_2	P_3
SRCP							
Global	52.0 ± 1.9	50.5 ± 1.8	49.2 ± 1.5	< 0.001	0.002	< 0.001	0.012
Inferior	51.7 ± 1.9	50.5 ± 1.7	49.6 ± 2.2	0.003	0.024	0.001	0.085
Nasal	51.8 ± 2.0	50.3 ± 2.0	49.2 ± 3.0	0.002	0.012	< 0.001	0.091
Superior	52.1 ± 2.1	50.5 ± 2.1	49.5 ± 2.2	0.001	0.008	< 0.001	0.106
Temporal	52.5 ± 2.0	50.6 ± 2.1	48.9 ± 2.8	< 0.001	0.003	< 0.001	0.007
DRCP							
Global	57.4 ± 2.2	54.8 ± 2.5	51.7 ± 2.2	< 0.001	< 0.001	< 0.001	< 0.001
Inferior	57.7 ± 2.4	54.8 ± 2.8	53.2 ± 2.8	< 0.001	< 0.001	< 0.001	0.033
Nasal	57.2 ± 2.2	54.6 ± 2.5	52.4 ± 3.2	< 0.001	< 0.001	< 0.001	0.003
Superior	57.8 ± 2.4	55.2 ± 2.6	52.9 ± 2.8	< 0.001	< 0.001	< 0.001	0.002
Temporal	56.9 ± 2.4	54.5 ± 2.4	52.0 ± 3.4	< 0.001	0.001	< 0.001	0.001

SRCP, superficial retinal capillary plexus; DRCP, deep retinal capillary plexus. P^*, P value among the three groups; P_1, P value between control group and simple high myopia; P_2, P value between control group and pathological myopia; P_3, P value between simple high myopia and pathological myopia.

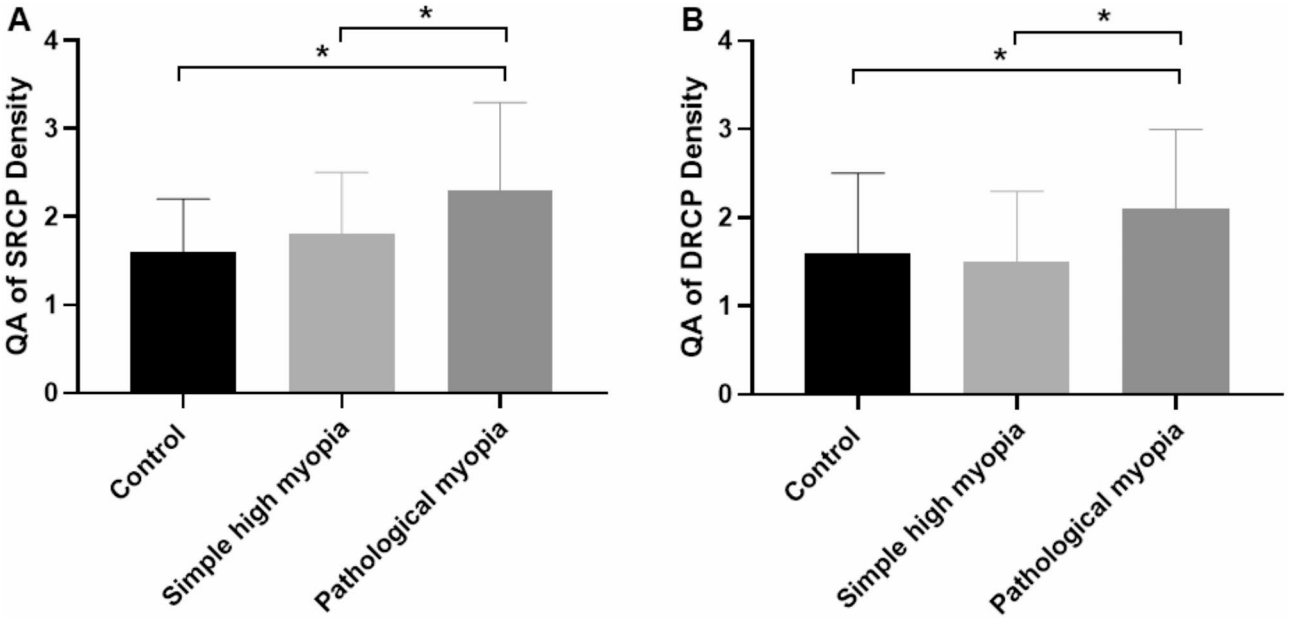

Fig. 2 Differences in quadrant asymmetry of retinal microvasculature density among the control, simple high myopia and pathological myopia. (**A**) QA of SRCP density among the three groups; (**B**) QA of DRCP density among the three groups. * indicated P-value less than 0.05. QA, quadrant asymmetry; SRCP, superficial retinal capillary plexuses; DRCP, deep retinal capillary plexuses

Differences in quadrant asymmetry of retinal microvasculature density among the control, simple high myopia and pathological myopia

For the QA value, there was a significant difference in QAs of SRCP and DRCP density among the three groups ($P = 0.024$ and 0.030, respectively). Simple high myopia didn't show any significant difference in QAs of SRCP and DRCP density when compared to the control (SRCP, 1.8 ± 0.7 vs. 1.6 ± 0.6, $P = 0.539$; DRCP, 1.5 ± 0.8 vs. 1.6 ± 0.9, $P = 0.765$; Fig. 2). The pathological myopia showed higher QAs of SRCP and DRCP density when compared to the control (SRCP, 2.3 ± 1.0 vs. 1.6 ± 0.6, $P = 0.012$; DRCP, 2.1 ± 0.9 vs. 1.6 ± 0.9, $P = 0.048$; Fig. 2) and simple high myopia (SRCP, 2.3 ± 1.0 vs. 1.8 ± 0.7, $P = 0.020$; DRCP, 2.1 ± 0.9 vs. 1.5 ± 0.8, $P = 0.010$; Fig. 2).

Comparing pathological myopia against control, the mean difference in QAs significantly differed for SRCP and DRCP density ($P = 0.010$ and 0.034, respectively, Table 3). Comparing pathological myopia against simple high myopia, the mean differences in QAs of SRCP and DRCP density were − 0.50 ± 0.23 and − 0.61 ± 0.23, respectively (Both $P \leq 0.015$, Table 3). Comparing simple high myopia against control, the mean difference in QAs of SRCP and DRCP density didn't show any significance (Both $P > 0.05$, Table 3).

Table 3 Comparison of QA with different permutations among the control, simple high myopia and pathological myopia

Parameters	Control vs. Simple high myopia		Controls vs. Pathological myopia		Simple high myopia vs. Pathological myopia	
	Mean difference in QA	*P*	Mean difference in QA	*P*	Mean difference in QA	*P*
SRCP	-0.13 ± 0.19	0.242	-0.63 ± 0.26	0.010	-0.50 ± 0.23	0.015
DRCP	0.07 ± 0.22	0.378	-0.54 ± 0.29	0.034	-0.61 ± 0.23	0.005

QA, quadrant asymmetry; SRCP, superficial retinal capillary plexus; DRCP, deep retinal capillary plexus.

Table 4 The binary logistic regression based on GEE analysis of the effect of QA of retinal microvasculature density on pathological myopia

	Univariate Regression				Multivariate Regression			
	β	Standard error	OR	*P*	β	Standard error	OR	*P*
SRCP	0.688	0.295	1.990	0.020	0.501	0.272	1.650	0.065
DRCP	0.831	0.322	2.300	0.010	0.688	0.326	2.000	0.035

GEE, generalized estimating equation; QA, quadrant asymmetry; SRCP, superficial retinal capillary plexus; DRCP, deep retinal capillary plexus; OR, Odds Ratio.

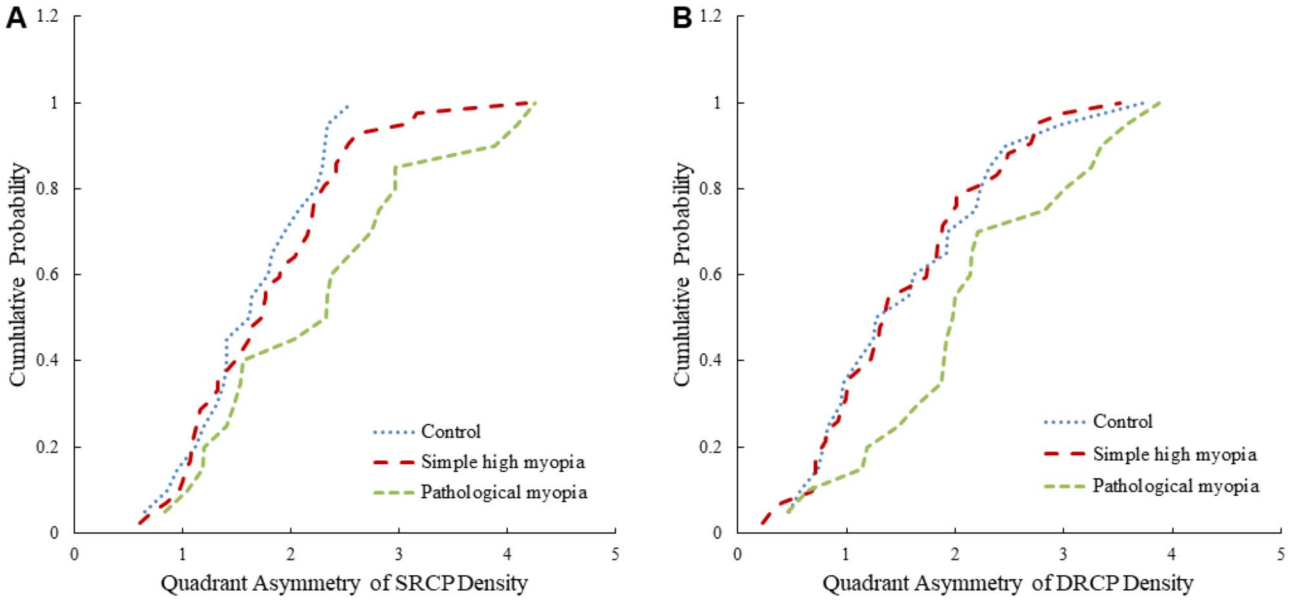

Fig. 3 Graph of the cumulative distribution function of QA among the control, simple high myopia and pathological myopia. (**A**) CDF plot showed that pathological myopia had greater QA of SRCP density than control and simple high myopia. (**B**) CDF plot showed that pathological myopia had greater QA of DRCP density than control and simple high myopia. CDF, cumulative distribution function; QA, quadrant asymmetry; SRCP, superficial retinal capillary plexuses; DRCP, deep retinal capillary plexuses

Effect of QA of retinal microvasculature density on pathological myopia

The binary logistic regression based on GEE analysis was used to compare the effect of QAs of SRCP and DRCP density on pathological myopia. In the univariate binary logistic regression, both QAs of SRCP and DRCP density showed high risks for pathological myopia (Odds Ratio = 1.990 and 2.300, respectively, both $P < 0.05$, Table 4). In the final multivariate binary logistic regression, only QA of DRCP density showed a high risk for pathological myopia (Odds Ratio = 2.000, $P = 0.035$, Table 4).

The cumulative distribution function plot showed the difference in the distribution of QA in control, simple high myopia and pathological myopia for densities of SRCP and DRCP (Fig. 3). The distribution for the pathological myopia was right-shifted relative to the simple high myopia and control for both QAs of SRCP and DRCP density, which indicated pathological myopia had QAs of SRCP and DRCP density that were higher relative to the control and simple high myopia throughout the distribution.

Effect of retinal microvasculature density in subfields on pathological myopia

The binary logistic regression based on GEE was used to compare the effect of retinal microvasculature density of SRCP and DRCP in respective four macular subfields on pathological myopia. In the multivariate binary logistic regression, DRCP density in the inferior area showed

Table 5 The binary multivariate logistic regression based on GEE analysis of the effect of retinal microvasculature density in four subfields on pathological myopia

	SRCP				DRCP			
	β	Standard error	OR	*P*	β	Standard error	OR	*P*
Inferior	-0.237	0.344	0.789	0.490	-0.832	0.385	0.435	0.030
Nasal	-0.192	0.282	0.825	0.498	-0.010	0.275	0.990	0.971
Superior	-0.024	0.254	0.976	0.926	0.716	0.383	2.046	0.061
Temporal	0.659	0.346	1.933	0.057	0.439	0.382	1.551	0.251

GEE, generalized estimating equation; SRCP, superficial retinal capillary plexus; DRCP, deep retinal capillary plexus; OR, Odds Ratio.

a high risk for pathological myopia (Odds Ratio = 0.435, $P = 0.030$, Table 5). The SRCP density in all four receptive subfields didn't show a risk for pathological myopia (All $P > 0.05$, Table 5).

Discussion

In the current study, we used OCTA to compare the QA changes in the retinal microvascular density of eyes with simple high myopia and with pathological myopia compared to the control in the macular area. Pathological myopia showed higher QAs of SRCP and DRCP density when compared to the control and simple high myopia. However, there was no significant difference in QAs of SRCP and DRCP density between the control and simple high myopia. The QA of DRCP density showed a high risk for the occurrence of pathological myopia. More interestingly, the decreased macular inferior DRCP density was sensitive to indicate pathological myopia.

With the development of high myopia, the decreasing densities of SRCP and DRCP had been reported previously [6, 8, 13, 14]. In our previous study, we had already found that the retinal microvasculature of high myopia was affected by diffuse changes instead of isolated local alterations [8, 13]. Whether the diffuse changes were similar in all isolated local subfields with the same steps in pathological myopia was unclear. By analyzing the microvascular density in control and high myopia, Li et al. found that retinal microvascular density in all macular subfields decreased in high myopia except in the superior-temporal area [7]. It might indicate the quadrant asymmetric changes in SRCP and DRCP for different subfields in high myopia. How the quadrant asymmetric changes in macular retinal microvascular density had been changed in high myopia, especially in pathological myopia, was still unclarified. In the current study, we used the QA to indicate the quadrant asymmetric changes in the macular retinal microvascular density. It had been reported that the parameter of QA could exclude the confounding effects of intra-eye variables and was more sensitive to indicate quadrant asymmetric alteration than using minimum/maximum flow density ratio or other related parameters [10–12]. To our knowledge, this was the first study to report the increased quadrant asymmetric changes in macular retinal microvascular density in pathological myopia, which was reflected by higher QAs of SRCP and DRCP density.

The higher QAs of SRCP and DRCP density occurred in pathological myopia. In our previous study, the quadrant asymmetric vessel density alteration occurred around the peripapillary area in pathological myopia [9]. As we had known, the large blood vessels around the peripapillary area sent the branches to the macular region as the SRCP and DRCP. With the occurrence of pathological myopia, there would be asymmetric loss of the macular retinal perfusion, leading to higher QA. We supposed the quadrant asymmetric changes in retinal microvascular density in both the macular and peripapillary areas in pathological myopia might be related to the axial elongation with the form of posterior scleral staphyloma. With the occurrence of pathological myopia and the forming of the posterior scleral staphyloma, the scleral stress might be regional differences [15, 16]. The mechanical scleral stress would be relieved by large disc tilt and other deformation in pathological myopia. The vulnerability of the macular area to mechanical stretch and scleral stress in pathological myopia would occur due to around 88% of posterior scleral staphyloma being involved in the macula [17]. Then, the local strain of the macular area might be relieved with decreasing vessel perfusion and related degeneration. The differences in local strain might lead to quadrant asymmetric alteration in the macular retinal microvascular density [15, 16].

The higher QA of DRCP density was a significant parameter to indicate the occurrence of pathological myopia when compared to the QA of SRCP density. The SRCP density might be less sensitive to change during the occurrence of pathological myopia for the SRCP was located mainly near the large retinal vessel [18, 19]. On the contrary, as the major vascular layers of the macula and the most vulnerable vascularity, the DRCP would be with higher asymmetric alteration with serious loss of density in pathological myopia [20–25]. The significant alteration of DRCP density rather than the SRCP density in pathological myopia had been reported previously [6]. With the occurrence of pathological myopia, the DRCP supplied more oxygen to the outer retina than control and simple high myopia [4]. For the decreased DRCP density and increased QA of DRCP density in

pathological myopia, the imbalanced vessels of blood occurred in the outer retina which might result in outer retinoschisis [26, 27]. As we had known, outer retinoschisis was the most common type of myopic foveoschisis and one of the most common complications of pathological myopia as well [28, 29]. Then we highlighted the importance and effectiveness of the QA of DRCP density in indicating the occurrence of pathological myopia.

Based on the analysis of the effect of retinal microvasculature density in subfields on pathological myopia, the decreased inferior DRCP density showed a higher risk of pathological myopia. Similarly, the decreased retinal density in the temporal-inferior peripapillary area showed the highest risk for pathological myopia when compared to other related peripapillary areas [9]. To compensate for the inferior ischemia in pathological myopia, the retinal vessels contracted seriously both in the peripapillary area and the macular area. The DRCP density in the inferior area would be sensitive to adjust for pathological myopia. Similarly, the patchy atrophy of pathological myopia more often occurred in the inferior area rather than the other areas [30]. We speculated that when serious pathological fundus occurred as pathological myopia, the significantly decreased retinal microvascular perfusion in this subfield would occur. However, the underlying mechanism of the frequently decreased inferior DRCP density in pathological myopia was still unclear. The inferior structure of the eyeball was weaker than other subfields which might just because this area was where the embryonic ocular fissure closed [31, 32]. It could also be related to the posterior scleral expansion and its corresponding stress in pathological myopia. As previously reported, greater expansion of the inferior sclera occurred when compared to other subfields [31]. Further study was needed to explore these underlying potentials. We supposed that the early detection of the DRCP density, especially in the inferior area, would be necessary to indicate pathological myopia in daily clinics.

In the current study, we still acknowledged some limitations. First, a larger sample size was needed to draw more reliable conclusions about the quadrant asymmetric alteration in the macular retinal microvascular density in pathological myopia. With a larger sample size, the pathological myopic patients might be classified in detail with different severity and more interesting results would be found in this way. All pathological myopia were with posterior scleral staphyloma in the current study. In the future, we would also like to investigate the type of posterior scleral staphyloma in pathological myopia, which would give us more detail about the underlying mechanism of the quadrant asymmetric alteration of the retinal microvasculature. Then, as a cross-sectional study, it was still a limitation in concluding the high risk for pathological myopia. A further follow-up study was needed in our future study.

Based on the above, our study was the first to demonstrate the quadrant asymmetric alterations of the macular retinal microvascular density in pathological myopia. The quadrant asymmetric alterations of the macular retinal microvascular density, especially the deep retinal microvasculature, were significantly associated with the occurrence of pathological myopia. The deep retinal microvasculature in the macular inferior subfield showed high sensitivity to indicate pathological myopia. Thus, alteration of deep retinal microvasculature, especially in the macular inferior subfield, should be paid a lot of attention to during the daily clinic for pathological myopia.

Acknowledgements
Thanks for the support from Qucheng Hong.

Author contributions
YS, JY were responsible for the data analysis and data acquirement. MS was responsible for the data analysis and supervised the research. FL and JY were responsible for the wring and designed the current research. All authors were responsible for the supervision of the manuscript.

Funding
This study is supported by research grants from the Natural Science Foundation of Zhejiang Province (Grant No. LQ21H120007).

Data availability
Data was available and would be given when it was required.

Declarations

Ethics approval and consent to participate
The study adhered to the tenets of the Declaration of Helsinki and was approved by the Ethics Committee of the Eye Hospital of Wenzhou Medical University. Written informed consent was obtained from all subjects.

Consent for publication
All authors agree to publish this manuscript and all patients included consent to publish this manuscript using their clinic information.

Competing interests
No conflicting relationship exists for any author.

Received: 4 July 2024 / Accepted: 14 March 2025
Published online: 28 March 2025

References

1. Sankaridurg P, Tahhan N, Kandel H, et al. IMI Impact of Myopia. Invest Ophthalmol Vis Sci. 2021;62(5):2.
2. Hayashi K, Ohno-Matsui K, Shimada N, et al. Long-term pattern of progression of myopic maculopathy: a natural history study. Ophthalmology. 2010;117(8):1595–611. 1611.e1-4.
3. Ohno-Matsui K, Kawasaki R, Jonas JB, et al. International photographic classification and grading system for myopic maculopathy. Am J Ophthalmol. 2015;159(5):877–e8837.
4. Liu HH, Xu L, Wang YX, et al. Prevalence and progression of myopic retinopathy in Chinese adults: the Beijing Eye Study. Ophthalmology. 2010;117(9):1763–8.
5. Saw SM. How blinding is pathological myopia? Br J Ophthalmol. 2006;90:525–6.

6. Ye J, Wang M, Shen M, et al. Deep retinal capillary plexus decreasing correlated with the outer retinal layer alteration and visual acuity impairment in pathological myopia. Invest Ophthalmol Vis Sci. 2020;61(4):45.
7. Li M, Yang Y, Jiang H, et al. Retinal microvascular network and microcirculation assessments in high myopia. Am J Ophthalmol. 2017;174:56–67.
8. Yang Y, Wang J, Jiang H, et al. Retinal microvasculature alteration in high myopia. Invest Ophthalmol Vis Sci. 2016;57(14):6020–30.
9. Ye J, Lin J, Shen M, et al. Reduced radial peripapillary capillary in pathological myopia is correlated with visual acuity. Front Neurosci. 2022;16:818530.
10. Jung JJ, Lim SY, Chan X, et al. Correlation of diabetic disease severity to degree of quadrant asymmetry in en face OCTA metrics. Invest Ophthalmol Vis Sci. 2022;63(9):12.
11. Jung JJ, Soh YQ, Sha P, et al. Effects of induced astigmatism on Spectral Domain-OCT Angiography quantitative metrics. Am J Ophthalmol. 2020;219:49–58.
12. Jung JJ, Yu DJG, Ito K, et al. Quantitative assessment of asymmetric choroidal outflow in pachychoroid eyes on ultra-widefield indocyanine green angiography. Invest Ophthalmol Vis Sci. 2020;61(8):50.
13. Wu Q, Chen Q, Lin B, et al. Relationships among retinal/choroidal thickness, retinal microvascular network and visual field in high myopia. Acta Ophthalmol. 2020;98(6):e709–14.
14. Liu M, Wang P, Hu X, et al. Myopia-related stepwise and quadrant retinal microvascular alteration and its correlation with axial length. Eye (Lond). 2021;35(8):2196–205.
15. Sung MS, Lee TH, Heo H, Park SW. Association between optic nerve head deformation and retinal microvasculature in high myopia. Am J Ophthalmol. 2018;188:81–90.
16. Vurgese S, Panda-Jonas S, Jonas JB. Scleral thickness in human eyes. PLoS ONE. 2012;7(1):e29692.
17. Ohno-Matsui K. Proposed classification of posterior staphylomas based on analyses of eye shape by three-dimensional magnetic resonance imaging and wide-field fundus imaging. Ophthalmology. 2014;121(9):1798–809.
18. Chen X, Rahimy E, Sergott RC, et al. Spectrum of retinal vascular diseases associated with paracentral acute middle maculopathy. Am J Ophthalmol. 2015;160(1):26–e341.
19. Kur J, Newman EA, Chan-Ling T. Cellular and physiological mechanisms underlying blood flow regulation in the retina and choroid in health and disease. Prog Retin Eye Res. 2012;31(5):377–406.
20. Moore J, Bagley S, Ireland G, et al. Three dimensional analysis of microaneurysms in the human diabetic retina. J Anat. 1999;194(Pt 1):89–100.
21. Bek T. Transretinal histopathological changes in capillary-free areas of diabetic retinopathy. Acta Ophthalmol (Copenh). 1994;72(4):409–15.
22. Balaratnasingam C, An D, Sakurada Y, et al. Comparisons between histology and optical coherence tomography angiography of the periarterial capillary-free zone. Am J Ophthalmol. 2018;189:55–64.
23. Rahimy E, Kuehlewein L, Sadda SR, Sarraf D. Paracentral acute middle maculopathy: what we knew then and what we know now. Retina. 2015;35(10):1921–30.
24. Yu PK, Balaratnasingam C, Cringle SJ, et al. Microstructure and network organization of the microvasculature in the human macula. Invest Ophthalmol Vis Sci. 2010;51(12):6735–43.
25. Yu S, Wang F, Pang CE, et al. Multimodal imaging findings in retinal deep capillary ischemia. Retina. 2014;34(4):636–46.
26. Li T, Wang X, Zhou Y, Feng T, Xiao M, Wang F. Paravascular abnormalities observed by spectral domain optical coherence tomography are risk factors for retinoschisis in eyes with high myopia. Acta Ophthalmol. 2018;96:e515–23.
27. Fragiotta S, Leong BCS, Kaden TR, et al. A proposed mechanism influencing structural patterns in X-linked retinoschisis and stellate nonhereditary idiopathic foveomacular retinoschisis. Eye (Lond). 2019;33:724–8.
28. Fujimoto M, Hangai M, Suda K, Yoshimura N. Features associated with foveal retinal detachment in myopic macular retinoschisis. Am J Ophthalmol. 2010;150(6):863–70.
29. Shinohara K, Tanaka N, Jonas JB, et al. Ultrawide-Field OCT to investigate relationships between myopic macular retinoschisis and posterior staphyloma. Ophthalmology. 2018;125(10):1575–86.
30. Du R, Fang Y, Jonas JB, et al. Clinical features of patchy chorioretinal atrophy in pathologic myopia. Retina. 2020;40(5):951–9.
31. Ohno-Matsui K, Akiba M, Modegi T, et al. Association between shape of sclera and myopic retinochoroidal lesions in patients with pathologic myopia. Invest Ophthalmol Vis Sci. 2012;53:6046–61.
32. Jiang R, Wang YX, Wei WB, et al. Peripapillary choroidal thickness in adult Chinese: the Beijing Eye study. Invest Ophthalmol Vis Sci. 2015;56(6):4045–52.

Publisher's note